

1 **Critical Assessment of Automatic Traffic Sign Detection Using 3D LiDAR Point Cloud Data**

2 **Chengbo Ai**

3 PhD Student

4 School of Civil and Environmental Engineering

5 Georgia Institute of Technology

6 210 Technology Cir. Savannah, GA 31407

7 Phone: (912) 966-7920 Fax: (912)966-7929

8 Email: [chengbo.ai@gatech.edu](mailto:chengbo.ai@gatech.edu)

9 **Yi-Chang (James) Tsai (corresponding author)**

10 Associate Professor

11 School of Civil and Environmental Engineering

12 Georgia Institute of Technology

13 210 Technology Cir. Savannah, GA 31407

14 Phone: (912) 963-6977 Fax: (912)966-7929

15 Email: [james.tsai@ce.gatech.edu](mailto:james.tsai@ce.gatech.edu)

16 Submission Date: 08/01/2011

17 Word Count: 4,029

18 Tables and Figures: 13

19 Total:  $4,029 + 13 \times 250 = 7,279$

20 **ABSTRACT**

21 Traffic signs are important roadside appurtenances that provide critical guidance to road users  
22 including regulations, destinations, and safety related information. Traffic signs need to be  
23 inventoried by transportation agencies for asset management and maintenance purposes.  
24 However, the traditional method of manually inventorying signs is dangerous, labor-intensive,  
25 and time-consuming. There is a need for a safer and more effective traffic sign inventory  
26 method. This paper is the first that critically assesses the use of an automatic method for traffic  
27 sign detection using 3D LiDAR point cloud data in support of traffic sign inventory. The  
28 contribution of this paper is three-fold: 1) it presents an automatic method for traffic sign  
29 inventory using 3D LiDAR point cloud data; 2) it critically assesses the performance of the  
30 presented method in terms of detection rate and false negative (FN)/false positive (FP); 3) it  
31 suggests the adequate parameter values to achieve a good traffic sign detection rate. Actual data,  
32 collected on Interstate 95 (major arterial) and 37<sup>th</sup> Street in Savannah, Georgia (local road), is  
33 used to assess the performance. Results show that the presented method can correctly detect  
34 94.0% and 91.4% of the traffic signs on both roadways, respectively, with less than 7 FP cases.  
35 The results demonstrate that the presented method using 3D LiDAR point cloud data is  
36 promising for providing an alternative for traffic sign inventory. Future research directions are  
37 recommended.

38

39 **INTRODUCTION**

40 Traffic signs are essential appurtenances in the transportation system. Traffic signs provide vital  
41 guidance to road users regarding traffic regulations, adequate warnings, destinations and  
42 traveling information, and temporary road conditions. It is essential for transportation agencies to  
43 inventory the traffic signs under their jurisdiction, so they know the locations and conditions of  
44 their signs. Manual traffic sign inventory methods are commonly used by most of transportation  
45 agencies, e.g. state departments of transportation (DOTs). It requires engineers to physically  
46 approach to traffic signs and collect corresponding attribute data. Spreadsheets (1) and handheld  
47 computers (2) are widely used for a manual inventory. This method is dangerous, labor-  
48 intensive, and time-consuming. There is a need to explore alternatives for a safer and more  
49 effective traffic sign inventory.

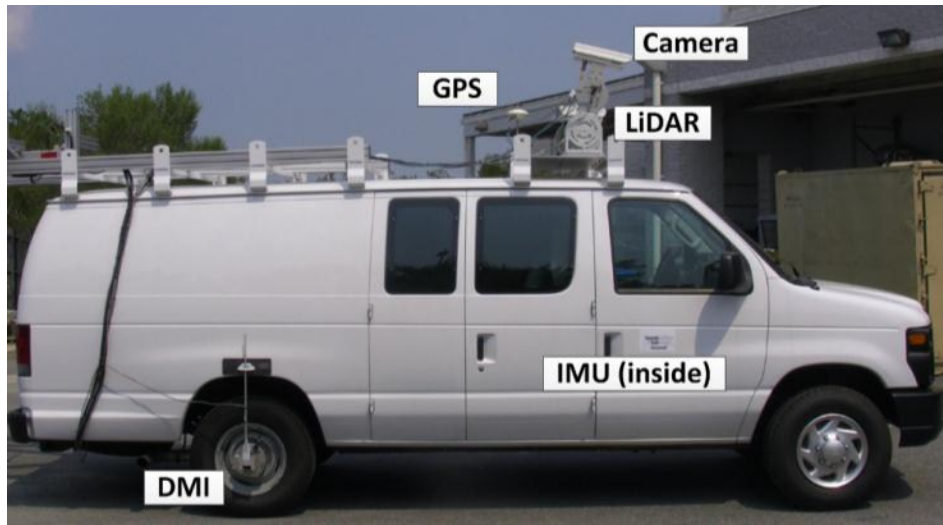
50 With the advancement of light detection and ranging (LiDAR) technology, terrestrial  
51 LiDAR has become popular in asset data collections (3-5). In recent years, mobile LiDAR data  
52 has been increasingly used for roadside inventory (6, 7). With accurate geo-referenced 3D point  
53 cloud data and the embedded unique retro-intensity information from the collected object, the  
54 LiDAR technology has the potential to achieve a safer and more effective traffic sign inventory.  
55 Although some researchers have attempted to use the LiDAR technology to collect traffic signs,  
56 a complete introduction of the method and the critical assessment on its performance is lacking.  
57 The objective of this study is to present an complete automatic traffic sign detection method  
58 using 3D LiDAR point cloud data and to conduct a critical assessment of its performance by  
59 using the actual data collected on Interstate 95 (I-95) and 37<sup>th</sup> Street in Savannah, Georgia (37<sup>th</sup>  
60 Street). Based on test outcomes, this study also suggests the adequate parameter values to  
61 achieve a good traffic sign detection performance.

62 This paper is organized as follows. The first section identifies the research need and  
63 objective. The second section presents an automatic traffic sign detection method using 3D  
64 LiDAR point cloud data. The third section presents the experimental test using actual data.  
65 Finally, conclusions and recommendations for the future research are discussed.

66 **AN AUTOMATIC TRAFFIC SIGN DETECTION METHOD USING 3D LIDAR POINT**  
67 **CLOUD DATA**

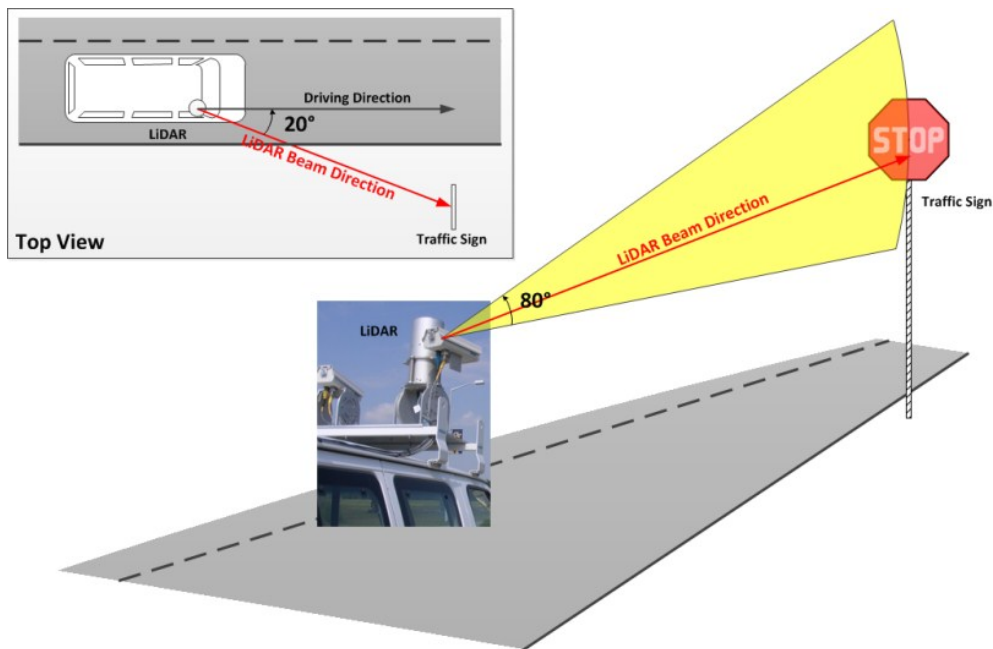
68 An automatic traffic sign detection method using 3D LiDAR point cloud data is presented in this  
69 section. Although there are some preliminary presentations on the use of 3D LiDAR data to  
70 collect traffic signs, this paper is the first to present a complete traffic sign detection method for  
71 traffic sign inventory.

72 The 3D LiDAR point cloud data is acquired using Georgia Tech’s mobile sensing system  
73 that can collect the data at highway speed. The integrated system includes the emerging mobile  
74 LiDAR system (i.e. Riegl LMS-Q120i), high resolution video cameras (i.e. Point Grey Gras-  
75 50S5C), and an accurate positioning system (i.e. Applanix LV 210PP) composed of a global  
76 positioning system (GPS), an inertial moment unit (IMU) and a distance measurement  
77 instrument (DMI), as shown in Figure 1.



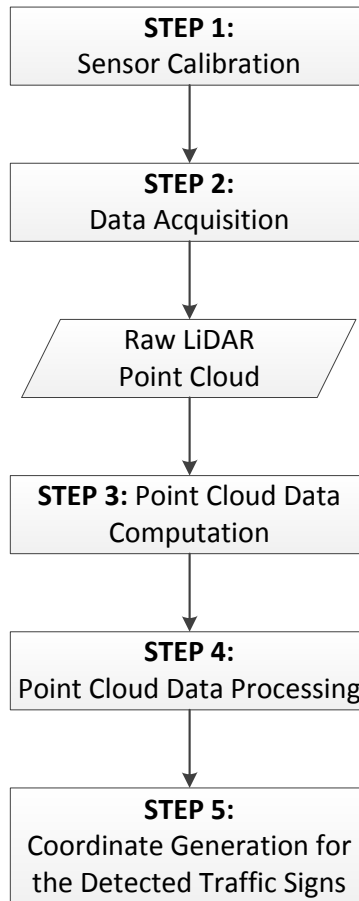
78  
79 **Figure 1 Georgia Tech’s mobile sensing system for collecting 3D LiDAR point cloud data**

80 The mobile LiDAR system in this study is a line-scanning laser device that produces  
81 10,000 laser points per second. As the vehicle moves in the longitudinal direction of the road,  
82 the scanning line of the LiDAR system is aligned perpendicularly to the ground. The scanning range  
83 is  $\pm 40^\circ$  to the horizontal direction, which produces an  $80^\circ$  fan covering the roadside. Currently,  
84 the frequency of the LiDAR system is configured at 100 Hz and 100 points within each scan,  
85 while the LiDAR heading angle is configured at  $20^\circ$ . Figure 2 shows an illustration of data  
86 acquisition. For example, if a standard  $48 \times 60$  speed limit sign is mounted on the roadside with a  
87 lateral offset of 12 ft. (3.6 m) to the edge of the road, the current configuration will be able to  
88 acquire a point cloud containing approximately  $12 \times 8$  points at 60 mph (100 km/h). The  
89 configuration can be adjusted to accommodate different data collection scenarios.



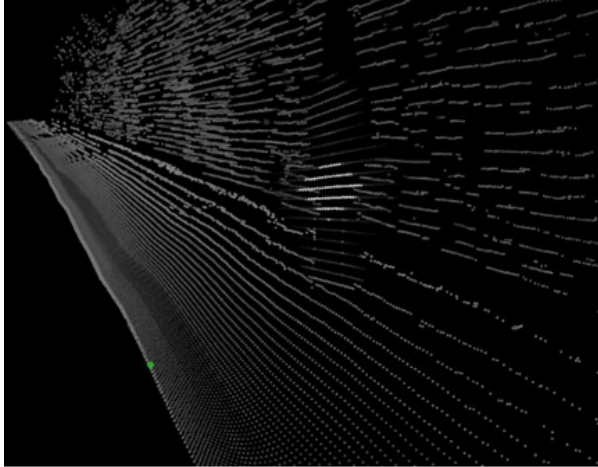
90  
91 **Figure 2 Illustration for data acquisition using LiDAR**

92 The new detection method contains five primary steps, including sensor calibration, data  
93 acquisition, point cloud data computation, point cloud data processing, and coordinate generation  
94 for the detected traffic signs. Figure 3 shows the flow of the traffic sign detection method using  
95 3D LiDAR point cloud data.



96  
97 **Figure 3 Flowchart of the traffic sign detection method using 3D LiDAR point cloud data**

98 **STEP 1:** Sensor calibration. For different sensor configurations, the system requires calibration  
99 of the LiDAR sensor to determine the positions (i.e. offsets in x, y, and z directions) and the  
100 actual poses (i.e. heading, rolling, and pitching angles) relative to the data collection system. The  
101 calibration results will be used for point cloud data computation. Sensor calibration needs to be  
102 conducted only when the sensor configuration is changed. In this study, the offsets of -6.0 inch (-  
103 15.3 cm), 16.1 inch (40.9 cm) and 21.8 inch (55.3 cm) for the x, y, and z directions, and the  
104 poses of 20°, 0°, and 1.2° for the heading, rolling, and pitching angles, are calibrated and used.  
105 **STEP 2:** Data acquisition. Once the sensors are calibrated, the data collection system can be  
106 driven on roadway for data collection. The 3D LiDAR point data can be collected and  
107 synchronized with the corresponding high resolution video log images (i.e. 2,448×2,048). Figure  
108 4 shows an example of the acquired data. Figure 4(a) shows the 3D LiDAR point cloud data.  
109 Figure 4(b) shows the corresponding video log image.



(a) 3D LiDAR point cloud data

(b) Video log image data

Figure 4 Example of the collected data on I-95

110  
111  
112

113 **STEP 3:** Point cloud data computation. After the data is acquired, the raw 3D LiDAR point  
114 cloud data and the corresponding raw GPS data are synchronized. The raw GPS data must be  
115 adjusted using the real-time IMU data, and it must be corrected using the differential base  
116 stations to obtain better accuracy. Using the sensor calibration results and the post-processed  
117 GPS data, the global coordinates for each point in the 3D point cloud can be accurately derived.

118 **STEP 4:** Point cloud data processing. The point cloud data are processed in three sub-steps for  
119 automatic traffic sign detection.

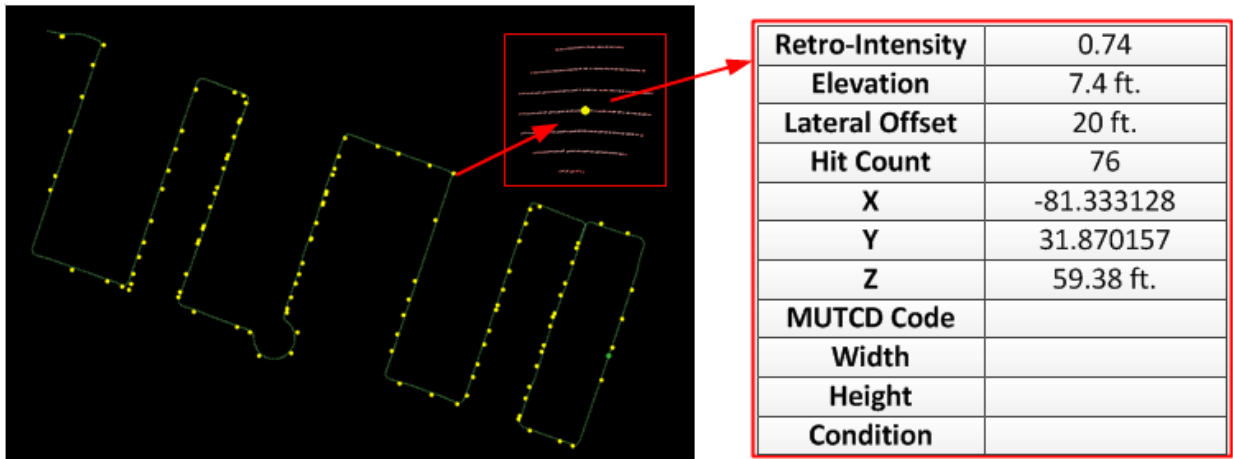
120 STEP 4.1: Point cloud filtering using retro-intensity. The retro-intensity is defined as the  
121 ratio of the energy returned from the object to the energy emitted from the LiDAR sensor. A  
122 higher retro-intensity indicates a better object reflectance. Since most of the traffic signs are  
123 designed to be retro-reflective, most of the traffic signs have a relatively high retro-intensity  
124 value in the LiDAR point cloud data compared to other objects. Using the retro-intensity  
125 parameter, only the clusters from the objects with high retroreflectivity will be filtered as the  
126 candidates for detected traffic signs.

127 STEP 4.2: Validate the clusters using geometrical constraints. Since traffic sign are  
128 standardized in the manual on uniform traffic control devices (MUTCD) for their locations  
129 and dimensions (8), these standards can be used for validating the clusters from STEP 4.1 to  
130 further remove the non-traffic sign clusters. In this study, the elevation, the lateral offset, and  
131 the hit count are used. The elevation parameter corresponds to the height of the traffic sign.  
132 The lateral offset parameter corresponds to the lateral location relative to the edge of the  
133 road. The hit count parameter is the number of LiDAR points that hit the cluster, which  
134 corresponds to the dimension of the traffic sign. A detailed analysis of how to determine the  
135 parameter values is presented in Section 3.

136 STEP 4.3: Determine the representative point. After the detected clusters are validated, the  
137 centroid of each cluster is used to represent the corresponding traffic sign. Within the  
138 centroid, the extracted attributes, e.g. the coordinates, the elevation, etc., corresponding to the  
139 detected traffic sign are embedded; other attributes, e.g. the MUTCD code, traffic sign  
140 dimension, etc., required for traffic sign inventory (9) can be filled in later.

141 **STEP 5:** Coordinate generation for the detected traffic signs. After the point cloud data is  
142 processed, the detected traffic signs are represented by a sequence of geo-referenced points (i.e.

143 the centroids for each detected traffic sign). A database can be generated containing the GPS  
 144 coordinates with the corresponding traffic signs and attributes. Figure 5 shows an example of the  
 145 detected traffic signs and the corresponding attributes on a geographic information system (GIS)  
 146 map. This step summarizes the complete automatic traffic sign detection method using 3D  
 147 LiDAR point cloud data.



148  
 149 **Figure 5 Example of the detected traffic sign and the corresponding attributes on GIS map**

150 Although the transportation agencies can use other commercially available software or  
 151 code their own application to implement the present method following similar steps, in our study,  
 152 functions from Trimble® Trident Analyst software are used to detect traffic signs.

153 **EXPERIMENTAL TEST**

154 The objective of the experimental test is to assess the performance of the presented automatic  
 155 traffic sign detection method using 3D LiDAR point cloud data. Actual data collected on I-95  
 156 and 37<sup>th</sup> Street is used to critically assess the performance of the presented method in terms of  
 157 detection rates and the FN and the FP. The adequate parameter values for a good detection rate  
 158 are also suggested.

159 The dataset collected on I-95 covers 17.5 miles of roadway containing 127 traffic signs  
 160 with different attributes. The data is collected on the outer lane of the three-lane road at the speed  
 161 of 60 mph (100 km/h). The dataset collected on 37<sup>th</sup> Street covers 2.9 miles of roadway  
 162 containing 115 traffic signs with different attributes. The data is collected at the speed of 30 mph  
 163 (50 km/h). Both of the datasets are collected using the same LiDAR heading angle of 20° and  
 164 scanning frequency of 100 Hz. The ground truth is manually extracted using the video log  
 165 images that are synchronized with the LiDAR data. Figure 6 shows the map of the road sections  
 166 for the data collection.

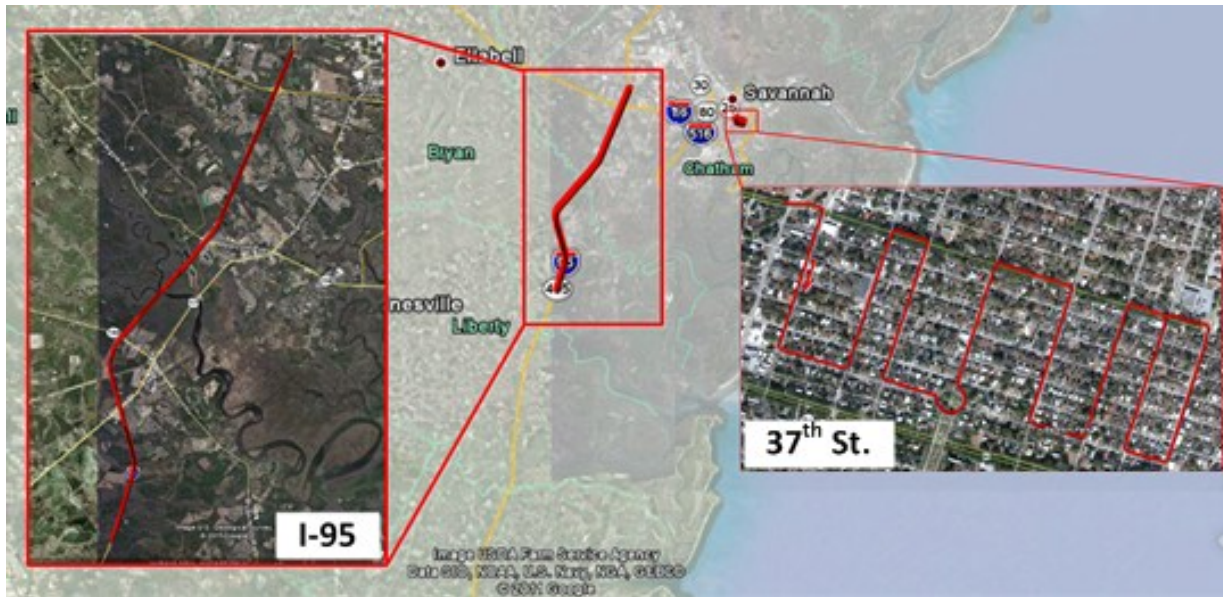


Figure 6 The selected data collection sections for experimental test

167  
168

### 169 Determination of Adequate Parameter Values

170 As presented in Section 2, the key parameters used for the presented method are related to the  
 171 basic traffic sign characteristics, such as the retroreflectivity, the elevation, etc. Therefore, the  
 172 initial parameter values can be set based on the MUTCD standard defining the traffic sign  
 173 characteristics. To adapt the traffic sign characteristics on different roadways, we have selected  
 174 the first 10 traffic signs on different roadway types to calibrate the parameter values. Once these  
 175 parameter values are calibrated, they can be applied to the same types of roadway. The following  
 176 rules are used to determine the adequate parameter values:

- 177 • Retro-intensity. The retro-intensity value selected for I-95 should be greater than that for 37<sup>th</sup>  
 178 Street. It indicates that the traffic sign retroreflectivity condition on the major arterials is  
 179 generally better than the local roads. On one hand, the retro-intensity value should be kept  
 180 low enough to prevent FN (i.e. missing signs). On the other hand, a higher retro-intensity  
 181 value is used to be selective on sign detection for minimizing the FP (i.e. false detection).  
 182 From the observation of the selected 10 traffic signs for calibration, the minimum retro-  
 183 intensity values of 0.73 are identified for I-95 and 0.67 for 37<sup>th</sup> Street. Therefore, values of  
 184 0.7 and 0.65 are used for I-95 and 37<sup>th</sup> Street, respectively.
- 185 • Elevation. The elevation value selected for I-95 should be slightly smaller than that for 37<sup>th</sup>  
 186 Street. It is consistent with the traffic sign installation standard defined in the MUTCD (8).  
 187 For example, although the traffic sign should be typically mounted at a minimum of 7 ft. (2.1  
 188 m) in height, many secondary signs can be mounted at a minimum of 5 ft. (1.5 m) on freeway  
 189 or expressway. Therefore, values of 4 ft. (1.2 m) and 6 ft. (1.8 m) are used for I-95 and for  
 190 37<sup>th</sup> Street, respectively. It is also suggested that the elevation value should not be smaller  
 191 than 3 ft. (0.9 m) to avoid the false detection of vehicle license plates and temporary traffic  
 192 control drums.
- 193 • Lateral Offset. The lateral offset value selected for I-95 should be greater than that for 37<sup>th</sup>  
 194 Street. It is consistent with the traffic sign installation standard defined in the MUTCD and  
 195 the observation in the calibration set. Based on the MUTCD, the traffic sign should be

196 mounted at a minimum of 12 ft. (3.6 m) lateral offset on freeway or expressway, whereas a  
 197 minimum of 2 ft. (0.6 m) lateral offset in residential area (8). However, as observed in the  
 198 calibration set, many specific service signs on the freeway or expressway are mounted as far  
 199 as 48 ft. off the road, while some of the traffic signs are mounted as far as 12 ft. (3.6 m) off  
 200 the road when the region is not confined. Therefore, values of 60 ft. (18.3 m) and 20 ft. (6.1  
 201 m) are used for I-95 and 37<sup>th</sup> Street respectively.

- 202 • Hit Count. The hit count value selected for I-95 should be smaller than that for 37<sup>th</sup> Street. As  
 203 presented in Section 2, the LiDAR point cloud data is collected using consecutive scanning  
 204 lines crossing the roadside objects. When the scanning frequency is fixed (i.e. 100 Hz), the  
 205 distance between the consecutive scanning lines is determined by the driving speed and the  
 206 distance between the consecutive points within the same line is determined by the distance  
 207 between the LiDAR sensor and the object. Therefore, a traffic sign with the same dimension  
 208 contains less hit points on I-95 than on 37<sup>th</sup> Street, because the vehicle speed for data  
 209 collection is greater, while the distance from the LiDAR to the traffic sign is also larger on I-  
 210 95 than on 37<sup>th</sup> Street. By exploring the smallest signs collected in the datasets on I-95 (i.e.  
 211 milepost sign) and on 37<sup>th</sup>, Street (i.e. no-parking sign) and based on the data collection  
 212 speeds, values of 10 and 20 are used for I-95 and for 37<sup>th</sup> Street, respectively.

213 The rules for determining adequate parameter values for the presented detection method are  
 214 based on the characteristics of traffic signs defined in the MUTCD and the calibration from a  
 215 fraction of the testing datasets. In this paper, the first 10 traffic signs are used for the calibration.  
 216 However, transportation agencies can define their fractions for better parameter values. Table 1  
 217 presents the selected parameter values used for the experimental test in this study.

218 **Table 1 The parameter values applied for the tests on I-95 and 37th Street**

I-95		37 <sup>th</sup> Street	
Retro-Intensity	0.70	Retro-Intensity	0.65
Min Elevation (ft.)	4	Min Elevation (ft.)	6
Max Lateral Distance (ft.)	60	Max Lateral Distance (ft.)	20
Min Hit Count	10	Min Hit Count	20

219 **Testing Results**

220 With the determined parameter values, the datasets collected on I-95 and 37<sup>th</sup> Street are tested  
 221 using the presented method. Table 2 shows the automatic detection results.

222 **Table 2 Traffic sign detection results for the tests on I-95 and 37th Street**

I-95		37 <sup>th</sup> Street	
Distance	17.5 miles	Distance	2.9 miles
# of Signs Tested	117	# of Signs Tested	105
Detection Rate	94.0%	Detection Rate	91.4%
False Negative	7	False Negative	9
False Positive	6	False Positive	7

223 For the data collected on I-95, the detection rate is 94.0% with only 6 FP cases. For the  
 224 data collected on 37<sup>th</sup> Street, the detection rate is 91.4% with only 7 FP cases. The results have

225 demonstrated that the presented method using 3D LiDAR point cloud data is promising for  
226 providing an alternative for traffic sign inventory.

227 The detailed analysis of the FN cases and FP cases are conducted. There are four types of  
228 FN cases: traffic signs with poor retroreflectivity condition, traffic signs with insufficient height,  
229 occluded traffic signs, and overhead traffic signs.

230 • Traffic sign with poor retroreflectivity condition. Several such FN cases are identified on 37<sup>th</sup>  
231 Street, where the retroreflectivity condition of the traffic signs is relatively poor. In contrast,  
232 this FN case is not identified on I-95, where the traffic signs are maintained in a timely  
233 manner. Figure 7 shows an example of a FN case containing a traffic sign with poor  
234 retroreflectivity condition on the 37<sup>th</sup> Street. It can be observed in the video log image that  
235 the no-parking sign has severely deteriorated. In the corresponding LiDAR point cloud data,  
236 the retro-intensity values of the points within the no-parking sign region are much smaller  
237 than the set parameter value of minimum retro-intensity as 0.65. Therefore, the traffic sign  
238 region will not be detected from the background. The further investigation finds that the  
239 average of the retro-intensity values in the traffic sign regions is approximately 0.45. By  
240 further reducing the parameter value of retro-intensity to below 0.45, this traffic sign can be  
241 correctly detected. However, many FP cases are detected using such a small retro-intensity  
242 parameter value.



243  
244 **Figure 7 Example of FN case with a traffic sign with poor retroreflectivity on 37<sup>th</sup> Street**

245 • Traffic sign with insufficient height. Several such FN cases are identified on 37<sup>th</sup> Street,  
246 where some of the traffic signs fail to meet the height requirements defined in the MUTCD.  
247 In contrast, this FN case is not identified on I-95, where the traffic signs have better  
248 compliance. Figure 8 shows an example of a FN case containing a traffic sign with  
249 insufficient height on 37<sup>th</sup> Street. The height of the traffic sign is measured as 5.1 ft. (1.6 m),  
250 which is smaller than the set parameter value of minimum elevation as 6 ft. (1.8 m).  
251 Therefore, the traffic sign region is rejected. By further reducing the parameter value of  
252 elevation to below 5 ft. (1.5 m), this traffic sign can be correctly detected. However, several  
253 additional FP cases are detected, such as the reflective stickers on the mailbox, etc.



254  
255

**Figure 8 Example of a FN case with a traffic sign with insufficient height on 37<sup>th</sup> Street**

- 256 • Occluded traffic sign. One of the drawbacks of the LiDAR point cloud data collection is that

257 only the object in the line of sight of the LiDAR sensor can be collected. Therefore, when the

258 heading of the LiDAR sensor is configured at a fixed angle (e.g. 20° in this study), the line of

259 sight is fixed. If the object closer to the LiDAR sensor is collected, the occluded object will

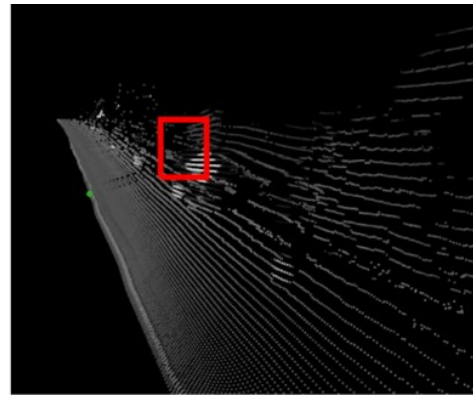
260 not be detected. Figure 9(a) shows an example of a FN case containing an occluded traffic

261 sign on I-95. The merge sign is occluded by the temporary work zone warning sign.

262 Although in the video log image, the merge sign is still visible, it cannot be detected using

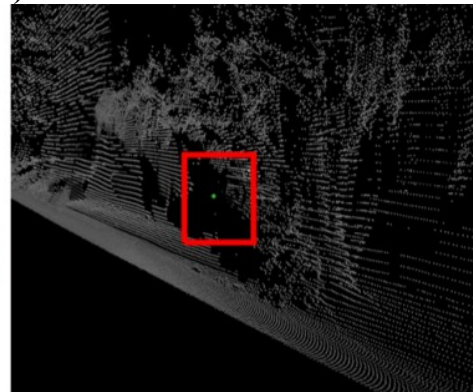
263 LiDAR point cloud data due to the occlusion. Similar cases are identified in the local road,

264 where traffic signs are occluded by the tree branches, as shown in Figure 9(b).



265  
266

(a)

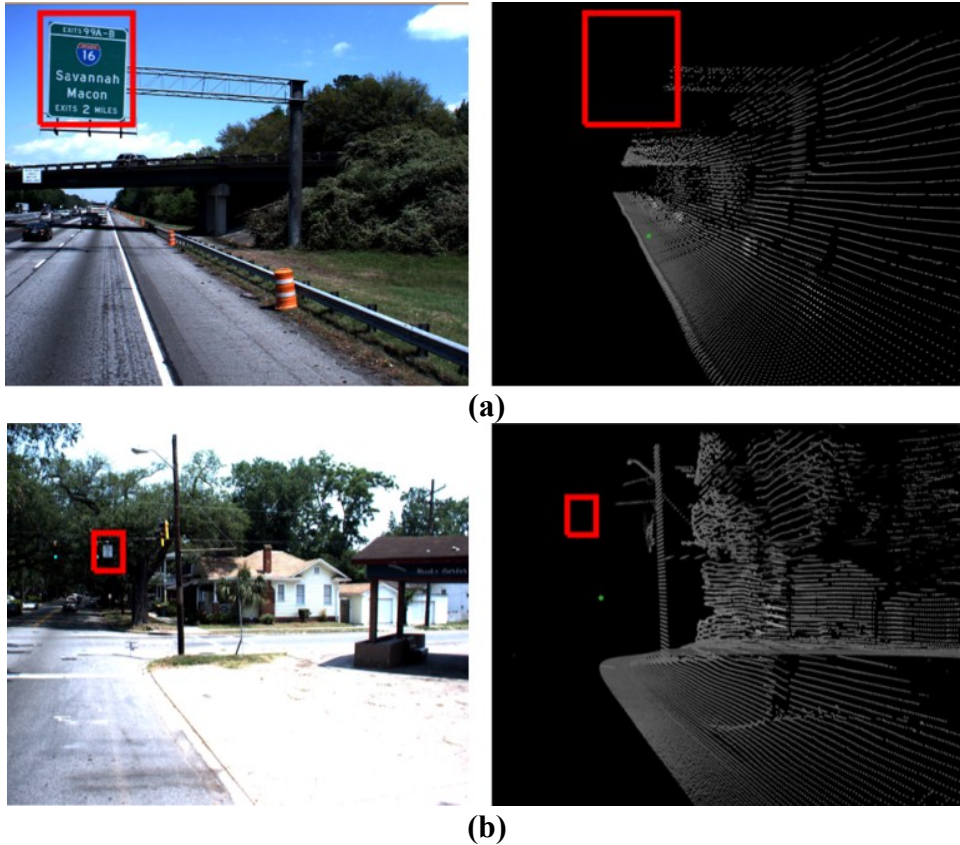


267  
268

(b)

269 **Figure 9 Example of FN cases containing occluded signs on (a) I-95 and (b) 37<sup>th</sup> Street**

- 270 • Overhead traffic sign. The coverage of the LiDAR data along the road is dependent on the  
271 path of the data collection vehicle and the heading angle of the LiDAR sensor (e.g. 20° in  
272 this study). For the purpose of traffic sign inventory, the LiDAR sensor is typically scanning  
273 vertically to the roadside and the data collection vehicle is driving on the outer lane of the  
274 road. Under such configuration, it is likely that many overhead signs are not detected. In  
275 contrast, the overhead signs can still be collected in the video log images. Figure 10 shows  
276 examples of such FN cases on I-95 and 37<sup>th</sup> Street.



279  
280  
281 **Figure 10 Example of FN cases containing overhead signs on (a) I-95 and (b) 37<sup>th</sup> Street**

282 There are three types of FP cases in which objects with high retroreflectivity are mistakenly  
283 detected as traffic signs. Although the constraint of traffic sign elevation effectively rejects many  
284 of the objects with high retroreflectivity, such as vehicle license plate, temporary traffic control  
285 drums, etc., there are still several types of FP cases that are difficult to be eliminated, including  
286 reflective commercial signs, changeable message boards, gates with reflective strips, etc. Figure  
287 11 shows the examples of the identified FP cases. It is observed that although these FP cases are  
288 mistakenly detected using 3D LiDAR point cloud data, they can be easily eliminated using the  
289 2D video log images.



(a) (b) (c)

**Figure 11 Examples of the identified FP cases**

290  
291  
292

293 In summary, the results from the data collection on I-95 and 37<sup>th</sup> Street have  
294 demonstrated the presented method using 3D LiDAR point cloud data is promising for providing  
295 an alternative for traffic sign inventory. The suggested rules for determining the adequate  
296 parameter values show its effectiveness for the presented method. The FN and FP cases are  
297 critically assessed to assist in exploring the potential improvements. Two of the identified FN  
298 cases can be further eliminated by adjusting the parameter values, e.g. the traffic signs with poor  
299 retroreflectivity condition and insufficient height, while the other two identified FN cases can be  
300 further eliminated by changing the LiDAR configuration, changing the data collection path, or  
301 integrating the presented method with the image-based method. The integration of the presented  
302 method with the image-based method can also help to eliminate the identified FP cases.

### 303 CONCLUSIONS AND RECOMMENDATIONS

304 Traffic signs are important appurtenances for the transportation system and provide vital  
305 guidance for the road users. It is essential for transportation agencies to inventory the traffic  
306 signs. Traditionally, manual traffic sign inventory methods, which are dangerous, labor-intensive  
307 and time-consuming, are used. This study presents an automatic traffic sign detection method  
308 using 3D LiDAR point cloud data. The performance of the presented method is critically  
309 assessed using the actual data collected on I-95 and 37<sup>th</sup> Street. The detection rate is presented,  
310 and the FN cases / FP cases are analyzed in detail. The results have demonstrated that it is a  
311 promising alternative for traffic sign inventory.

312 The followings summarize the major findings of this study.

- 313 • Based on the test results, it has demonstrated that the presented traffic sign detection method  
314 using 3D LiDAR point cloud data has a good traffic sign detection rate. The result from the  
315 data collected on I-95 shows a slightly better detection rate than the one on 37<sup>th</sup> Street  
316 because the traffic signs on major arterials are likely to have better retroreflectivity  
317 conditions and are mounted in much better compliance with the MUTCD standard,  
318 comparing with the ones on local roads.
  - 319 ○ Based on the test conducted on I-95, the detection rate is 94.0% (110 correctly  
320 detected signs) with only 6 FP cases. The occluded traffic signs and overhead traffic  
321 signs are identified as the primary FN cases in this dataset.
  - 322 ○ Based on the test conducted on 37<sup>th</sup> Street, the detection rate is 91.4% (96 correctly  
323 detected signs), with only 7 FP cases. The traffic signs with poor retroreflectivity

324 condition and traffic signs with insufficient height are identified as the primary FN  
325 cases in this dataset.

- 326 • Based on the results, the current selections of parameter values, including the retro-intensity,  
327 the elevation, the lateral offset and the hit count, are adequate for the presented automatic  
328 traffic sign detection method. The rules for determining these parameter values show its  
329 effectiveness.
- 330 • Based on the results, the current LiDAR configuration (i.e. 20° heading angle and 100 Hz  
331 scanning frequency) and the data collection driving speed (i.e. 60 mph (100 km/h) for I-95  
332 and 30 mph (50 km/h) for 37<sup>th</sup> Street) are adequate for the presented automatic traffic sign  
333 detection method.

334 The followings are recommended for future research.

- 335 • Additional datasets for roadways with traffic signs having different attributes, e.g. condition,  
336 type, dimension, location, etc., are recommended to further assess the performance of the  
337 presented method.
- 338 • Further adjustments of parameter values are recommended to eliminate the FN cases,  
339 including the traffic signs with poor retroreflectivity condition or insufficient height, without  
340 introducing excessive FP cases.
- 341 • The integration of 2D video log image and 3D LiDAR point cloud data is recommended to  
342 further eliminate the FN cases, including the occluded signs and the overhead signs, and the  
343 FP cases, including the changeable message board, the reflective strip, etc.

#### 344 **ACKNOWLEDGEMENTS**

345 This study was sponsored by US department of transportation (US DOT) research innovative  
346 technology administration (RITA) program (DTOS59-10-H-0003). The authors would like to  
347 thank the support provided the US DOT RITA program. The author would also like to thank the  
348 technical assistance provided by the Trimble<sup>®</sup> GeoSpatial department. This paper only represents  
349 the opinion from the Georgia Tech research team and it does not necessarily represent the  
350 opinion of the USDOT.

#### 351 **REFERENCE**

- 352 1. Wolshon, B. *Louisiana Traffic Sign Inventory and Management System Report-381*.  
353 Publication LTRC Project No. 01-1SS, Baton Rouge, 2003.
- 354 2. Paoly, D. and A. B. Staud. Use of Mobilegis for Sign Inventories. *AASHTO GIS for*  
355 *Transportation*, 2010.
- 356 3. Hiremagalur, J., K. Yen, T. Lasky and B. Ravani. Testing and Performance Evaluation of  
357 Fixed Terrestrial Three-Dimensional Laser Scanning Systems for Highway Applications. *In*  
358 *Transportation Research Record: Journal of the Transportation Research Board*, Vol. 2098,  
359 No.1, 2009, pp. 29-40.
- 360 4. Al-Turk, E. and W. Uddin. Infrastructure Inventory and Condition Assessment Using  
361 Airborne Laser Terrain Mapping and Digital Photography. *In Transportation Research*  
362 *Record: Journal of the Transportation Research Board*, Vol. 1690, No.1, 1999, pp. 121-125.
- 363 5. Veneziano, D., R. Souleyrette and S. Hallmark. Integration of Light Detection and Ranging  
364 Technology with Photogrammetry in Highway Location and Design. *In Transportation*  
365 *Research Record: Journal of the Transportation Research Board*, Vol. 1836, No. 1, 2003,  
366 pp. 1-6.

- 367 6. Wende, Z. LiDAR-Based Road and Road-Edge Detection. *Intelligent Vehicles Symposium*  
368 *(IV)*, 2010 *IEEE*, 2010, pp. 845-848.
- 369 7. Laflamme, C., T. Kingston and R. McCuaig. Automated Mobile Mapping for Asset  
370 Managers. *Shaping the Change XXIII FIG Congress*, 2006,
- 371 8. FHWA. Manual on Uniform Traffic Control Devices for Streets and Highways 2009 Edition  
372 (MUTCD 2009). 2009.
- 373 9. McGee, H. W. *Maintenace of Signs and Sign Support: A Guide for Local Highway and Street*  
374 *Maintenance Personnel*. Washington D.C., 2010.